THE JOURNAL OF PHYSICAL CHEMISTRY Letters

Letter

pubs.acs.org/JPCL

The Role of Confined Water in Ionic Liquid Electrolytes for Dye-Sensitized Solar Cells

Jiwon Jeon,[†,⊥] Hyungjun Kim,*[,†,⊥] William A. Goddard, III,*[,†,‡,∥] Tod A. Pascal,[†,‡] Ga-In Lee,[§] and Jeung Ku Kang[†,§,∥]

[†]Graduate School of Energy Environment Water Sustainability (EEWS), Korea Advanced Institute of Science and Technology, Daejeon, 305-701, Republic of Korea

[‡]Materials and Process Simulation Center, Beckman Institute, California Institute of Technology, Pasadena, California 91125, United States

[§]Materials Science, Korea Advanced Institute of Science and Technology, Daejeon, 305-701, Republic of Korea

[∥]World Class University (WCU) Project, EEWS, Korea Advanced Institute of Science and Technology, Daejeon 305-701, Republic of Korea

Supporting Information

ABSTRACT: Ionic liquids (ILs) provide an attractive medium for various chemical and redox reactions, where they are generally regarded as hydrophobic. However, Seddon et al. discovered that 4−10 wt % water absorbs into ILs that contain bulky anions, and Cammarata et al. found that the molecular state of water in ILs is dramatically different from that of bulk liquid water or that of water vapor. To determine the microstructure of water incorporated into ILs and the impact on properties, we carried out first-principles-based molecular dynamics simulations. We find water in three distinct phases depending on water content, and that the transport properties depend on the nature of the water phases. These results suggest that the optimal water content is ∼10% mole fraction of water molecules (∼1.1 wt %) for applications such as nonvolatile electrolytes for dye-sensitized solar cells (DSSCs). This suggests a strategy for improving the performance of IL DSSC by replacing water with additives that would play the same role as water (since too much water can deteriorate performance at the anode−dye interface).

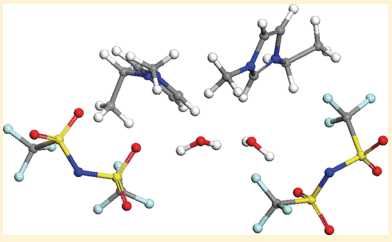

SECTION: Molecular Structure, Quantum Chemistry,General Theory

The dye-sensitized solar cell (DSSC) proposed by Grätzel et al.[1] is a promising candidate for photovoltaic devices because of low-cost and high efficiency. These systems involve a dye such as $[RuL_2(NSC)_2]_2$:TBA (L = 2,2′-bipyridyl-4,4′-dicarboxylic acid; TBA = tetra-*n*-butylammonium) attached to a TiO_2 anode in an electrolyte suitable for transporting the reductant (I^-/I_3^-). The reductant reduces the dye to its initial state following photo excitation and injection of the excited electron into the TiO_2 anode. DSSCs utilizing acetonitrile organic solvents as the electrolyte lead to the best energy conversion efficiency (∼11%);[2] however, long-term stability is limited by high volatility. Ionic liquids (ILs) provide a promising alternative,[3,4] since they are nontoxic,[5] nonvolatile, and nonflammable. However, with current ILs, the DSSC performance is degraded due to decreased reductant rates, presumably due to the high IL viscosity (39 mPa·s vs 0.34 mPa·s for acetonitrile).[6] To provide a basis for understanding how to improve the performance of IL-based DSSCs, we carried out atomistic simulations for all processes involved in these devices. Here we report the development of a first principles-based force field (FF) for describing the structures and dynamics of reductants within a typical DSSC IL consisting of 1-ethyl-3-methyl imidazolium cation ($EMIm^+$) and trifluoromethane-sulfonyl-imide anion ($TFSI^-$).

$TFSI^-$-based ILs are commonly regarded as hydrophobic;[7−12] however, coulombmetric Karl Fischer titration showed that ILs absorb significant amounts of water (∼7 mol %) from the atmosphere.[12] The presence of water in ILs is expected to modify the transport properties, which should affect DSSC efficiency.[13] However, the effect of water on the microstructure and the impact on transport properties has not been established.[14,15] Here we report the effect of water on the microstructure, thermodynamics, and kinetics for IL electrolytes relevant for DSSCs. Moreover, improving the transport properties of the IL-based electrolyte by mixing with other solvents is of interest to the proper design of electrolyte for the DSSC.[16]

A typical IL electrolyte for DSSCs consists of 0.50 mol fraction of $EMIm^+$, 0.36 mol fraction of $TFSI^-$, 0.13 mol fraction of I^-, and 0.01 mol fraction of I_3^-.[10,17,18] Our simulations consider a cubic periodic cell with sides of ∼4 nm, leading to 180 $EMIm^+$, 130 $TFSI^-$, 45 I^-, and 5 I_3^- per cell (360 molecules with 5430 atoms). To examine the effect of water content on the IL-based electrolyte, we considered 0−

Received: January 3, 2012
Accepted: February 3, 2012
Published: February 3, 2012

25% mole fraction (χ_{WAT}) of water molecules (0−120 per simulation cell or up to 3.3 wt %).

As described in the Supporting Information, we optimized an FF to reproduce accurate quantum mechanics (QM) and then used this FF in molecular dynamics (MD) simulations. We first equilibrated the IL system using a procedure based on the cohesive energy density (CED) model.[19] Then, we calculated the thermodynamic properties from the vibrational density of states (DoS) extracted from the MD using the two-phase thermodynamics (2PT) method.[20]

Figure 1 shows the average coordination of each species to water (CN) as a function of water content (using cutoff

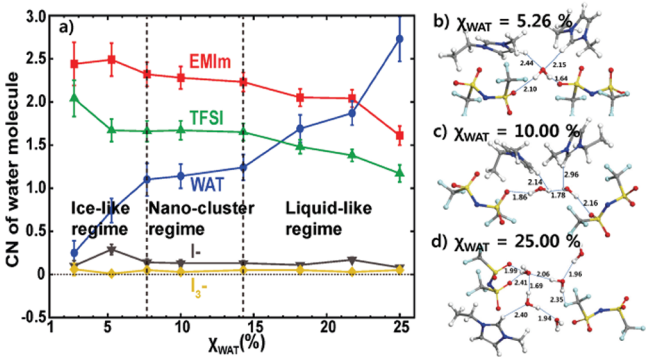

Figure 1. (a) Dependence of water coordination (CN) on the water molar content (χ_{WAT}). The $EMIm^+$ (red) and $TFSI^-$ (green) CN decrease with increasing χ_{WAT}, while water−water interactions (blue) increase with χ_{WAT}. Representative water structure mediating $EMIm^+$−$TFSI^-$ interactions after 30 ns MD for (b) the ice regime, χ_{WAT} = 5.26%, (c) the nanocluster regime, χ_{WAT} = 10.00%, and (d) the liquid-like regime, χ_{WAT} = 25.00%.

distances of 1.25 times the van der Waals contact distances). The waters interact mainly with $TFSI^-$, $EMIm^+$, and with other water molecules, but not with I^- or I_3^- ions.

We find that the molecular state of water in the IL system exhibits three regimes depending on H_2O content:

- *Ice-like regime* (χ_{WAT} < 7.69%): Each water molecule is coordinated by ∼1.8 $TFSI^-$ and ∼2.4 $EMIm^+$, but less than one water. The waters are mostly isolated and intercalated in between two $EMIm^+$ and two $TFSI^-$ (Figure 1b), leading to an entropy similar to ice.
- *Nano-cluster regime* (χ_{WAT} = 7.69−14.29%): Each water is coordinated to ∼1.2 water molecules, 1.7 $TFSI^-$, and 2.3 $EMIm^+$. This nanosized water cluster bridges between two $EMIm^+$ and two $TFSI^-$ (Figure 1c).
- *Liquid-like regime* (χ_{WAT} = 14.29−25.00%): Here the average water coordination increases to 2.7, leading to clusters with several waters located between $EMIm^+$ and $TFSI^-$ ions. The water−$TFSI^-$ coordination decreases to 1.2, and the water−$EMIm^+$ coordination decreases to 1.6. (Figure 1d). $EMIm^+$−$TFSI^-$ interactions are efficiently screened by the multiple waters, lubricating the motions of bulky ionic species in IL.

Figure 2 shows that

- In the ice-like regime, ∼80% to 40% of the water clusters are monomers.
- In the nano-cluster regime, the fraction of water remaining isolated water stays at ∼33%, while the average water cluster has two waters.

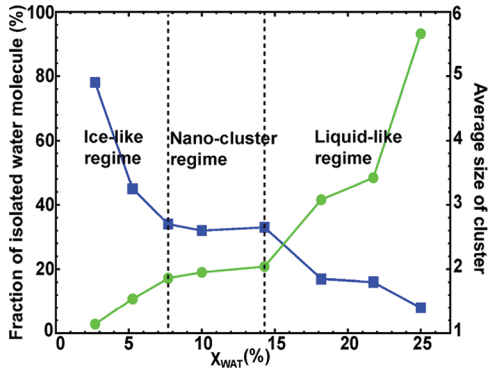

Figure 2. Fraction of isolated water molecule (blue) and the average cluster size (green) as a function of water content (χ_{WAT}). The number of waters in each cluster increases with increasing of χ_{WAT}. From previous IR experimental study,[12] the water molecule in the similar IL system ($BMIm^+$/$TFSI^-$) with ∼7 mol % shows IR peak splitting of symmetric and antisymmetric stretching modes, inferring that the water in this water content regime is isolated and very different from liquid phase water. This compares with our simulation results.

- In the liquid-like regime, the fraction of isolated waters decreases from 20 to 8%, and the average size of water cluster increases up to 5.66.

These results can be compared to IR experiments on the IL composed of 1-butyl-3-methyl imidazolium ($BMIm^+$) with $TFSI^-$, which concluded that water in χ_{WAT} ∼7 mol % is isolated, with a character distinct from the bulk liquid phase.[12]

To determine how this water-induced change in microstructure affects the thermodynamics, we evaluated the Helmholtz free energy ($A°$), entropy ($S°$), and enthalpy ($E°$) from the quantum distribution of vibrational states extracted from MD using the 2PT method. The changes of $A°$, $S°$, and $E°$ as a function of water content are shown in Figure S3, from which the slope leads to the water chemical potential ($\mu°_{WAT} = \partial A°/\partial n_{wat}$) with entropic ($\sigma°_{WAT} = \partial S°/\partial n_{wat}$) and enthalpic contributions ($\varepsilon°_{WAT} = \partial E°/\partial n_{wat}$) to $\mu°_{WAT}$ (where n_{wat} denotes the number of water molecules and $\mu°_{WAT} = \varepsilon°_{WAT} - T\sigma°_{WAT}$). Most interesting here is the dependence of the water chemical potential ($\mu°_{WAT}$) on χ_{WAT} as shown in Figure 3.

- *Ice-like regime*: $\mu°_{WAT}(IL)$ = −34.17 kJ/mol. Water bridges between $EMIm^+$ and $TFSI^-$ ions, leading to a more favorable enthalpy than for gas phase water ($\varepsilon°_{WAT}(IL) < \varepsilon°_{WAT}(g)$). However, these isolated waters have very low entropy, comparable to the entropy of ice ($s°_{WAT}(IL) \sim s°_{WAT}(s)$). Such exceptionally low entropy of water is originated by the isolated water molecule strongly bound to the $EMIm^+$ and $TFSI^-$ ions as shown in Figure 1b. The net result is that $\mu°_{WAT}(IL) > \mu°_{WAT}(g)$, so water in the regime has a chemical potential higher than the vapor.
- *Nano-cluster regime*: $\mu°_{WAT}(IL)$ = −45.54 kJ/mol, which is approximately half way between bulk water and water vapor (−41.61 kJ/mol). The additional water molecule neighbors increases the mobility of the electrolytes (Figure S6) by screening the huge electrostatic interactions among ionic species. Thus, $s°_{WAT}(IL)$ in the nanocluster regime is much larger than that in the ice-like regime. Here the enthalpic and entropic thermodynamic forces both favor the water absorption into IL ($\mu°_{WAT}(IL) < \mu°_{WAT}(g)$).

dx.doi.org/10.1021/jz3000036 | J. Phys. Chem. Lett. 2012, 3, 556−559

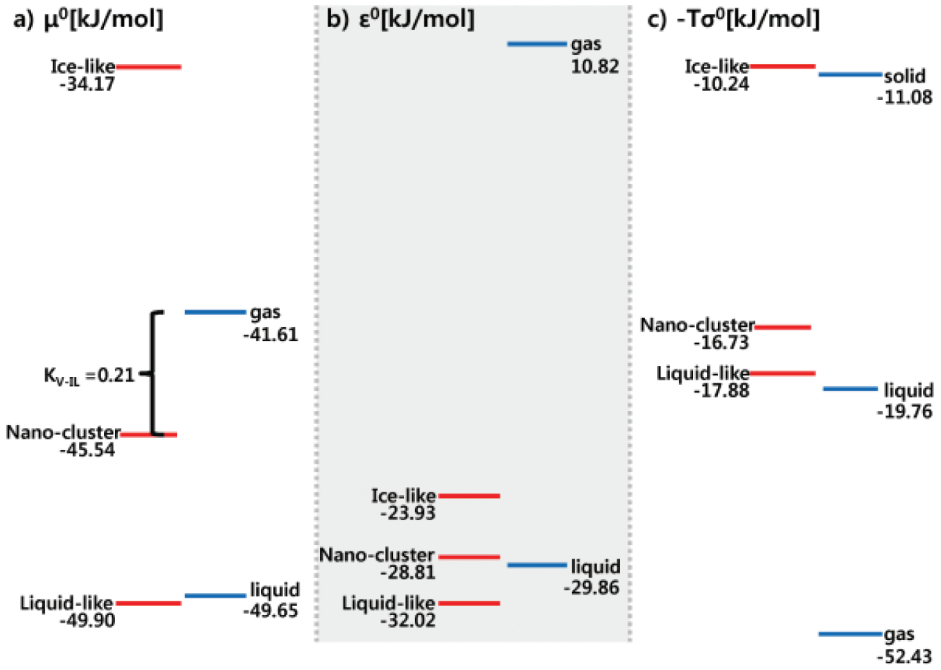

Figure 3. The thermodynamics for various water content regimes at standard temperature and pressure (STP) conditions. The red lines are for water in the IL. The blue lines are for water vapor (denoted as gas), bulk water (denoted as liquid), and ice (denoted as solid). (a) $\mu^{\circ}_{WAT(IL)}$ (= $\partial A^{\circ}/\partial n_{WAT}$) in the ice-like regime is higher than that for vapor water. $\mu^{\circ}_{WAT(IL)}$ in the nanocluster regime is between $\mu^{\circ}_{WAT(gas)}$ and $\mu^{\circ}_{WAT(liquid)}$. This leads to $K_{V\text{-}IL}$ = 0.21 vapor−IL equilibrium constant. The $\mu^{\circ}_{WAT(IL)}$ in the liquid-like regime is similar to $\mu^{\circ}_{WAT(liquid)}$. (b) $\varepsilon^{\circ}_{WAT(IL)}$ (= $\partial E^{\circ}/\partial n_{WAT}$) is more stable than $\varepsilon^{\circ}_{WAT(gas)}$ by 33−42 kJ/mol, which is comparable to the experimental value of 25−39 kJ/mol.[26] (c) $\sigma^{\circ}_{WAT(IL)}$ (= $\partial S^{\circ}/\partial n_{WAT}$) is lower than $\sigma^{\circ}_{WAT(gas)}$ by 115−140 J/mol·K, which is comparable to experiment: 102−135 J/mol·K.[26]

- *Liquid-like regime*: μ°_{WAT}(IL) = −49.90 kJ/mol, which is close to the chemical potential of −49.65 kJ/mol for liquid water.

These chemical potentials suggest that at 60−70% humidity, the amount of absorbed water is χ_{WAT} = 9−10.5% (see Supporting Information). Considering that the shorter chain imidazolium based IL absorbs more water than the longer chain imidazolium-based IL,[9,11] our value is consistent with the experimental result of 7 mol % from Karl Fischer titration on $BMIm^+$-type ILs with $TFSI^-$.[12]

To examine the effect of water absorption on transport properties of the IL, we examined the self-diffusion coefficient from the DoS(ν), at ν = 0 from the Green−Kubo relation. The center-of-mass translational diffusion coefficient of water D_{WAT}(trns.) in Figure S5a shows that the mass-transport of water molecules in IL is immobilized until the nanocluster regime. We find that addition of up to ∼10 mol % water enhances the diffusivity of $EMIm^+$ and $TFSI^-$ with marginal changes in the diffusivity of I^- and I_3^- (Figure S6). This is plausible since the water interacts primarily with $EMIm^+$ and $TFSI^-$ rather than I^- and I_3^- (Figure 1), resulting in more efficient dielectric screening of $EMIm^+$ and $TFSI^-$ by water molecules.

However, we find that I^- and I_3^- are coordinated by several $EMIm^+$ [∼6.4 $EMIm^+$ and ∼0.1 $TFSI^-$ for I^- and ∼7.1 $EMIm^+$ and ∼1.6 $TFSI^-$ for I_3^- (Figure 4)]. Since small amounts of H_2O increase the entropy and mobility of $EMim^+$ (Figure S4), we expect increased local fluctuations in I^- and I_3^-, which should increase the rate of Grotthuss-like electron transfer,[21] increasing the rate for reducing the oxidized dye. This would decrease the time available for electron−hole recombination; thereby improving performance of the DSSC. On the other hand, we expect that the large water clusters of the liquid-like

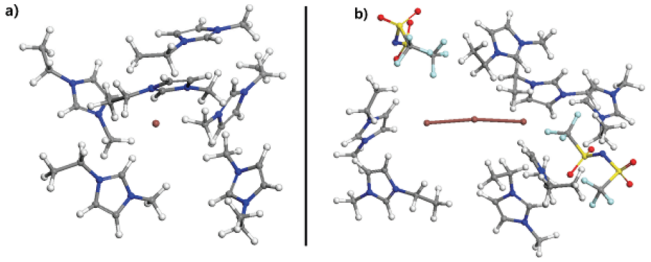

Figure 4. (a) I^- and (b) I_3^- surrounded by ILs for χ_{WAT} = 0 after 30 ns MD.

regime might allow water to access the TiO_2 interface. Since water (another Lewis base) is known to weaken the Lewis acid/base interaction of carboxylic group of dye molecules with the TiO_2 anode by competitively interacting with five-coordinated surface Ti atoms, and since close contact between dye and TiO_2 is essential to minimize the time for electron transfer from the photoexcited dye to the electrode, we expect that the large water clusters of the liquid-like regime would degrading photovoltaic performance.[22−25] Thus, we conclude that the nanocluster regime (7.69−14.29 mol %) may provide the best performance, allowing

(1) spontaneous absorption into the IL (μ°_{WAT}(IL)< μ°_{WAT}(l)),
(2) retention in the IL phase by binding as nanoclusters to $EMim^+$ or $TFSI^-$ ions, and
(3) lubricating fluctuations in the IL to enhance Grotthuss electron transport.

This suggests that a strategy for improving the performance of IL DSSCs by additives would play the same role as water

dx.doi.org/10.1021/jz3000036 | J. Phys. Chem. Lett. 2012, 3, 556−559

(since too much water can deteriorate performance at the anode−dye interface).

■ ASSOCIATED CONTENT

Ⓢ Supporting Information

Simulation and calculation details, comparison of QM and FF with optimized FF parameters, and detailed thermodynamic and diffusivity data are available free of charge via the Internet at http://pubs.acs.org.

■ AUTHOR INFORMATION

Corresponding Author

*linus16@kaist.ac.kr (H.K.); wag@wag.caltech.edu (W.A.G.).

Author Contributions

⊥These authors contributed equally.

Notes

The authors declare no competing financial interest.

■ ACKNOWLEDGMENTS

This work is supported by the WCU program (R31-2008-000-10055-0) of Korea; the generous allocation of computing time from the KISTI supercomputing center (KSC-2011-G1-01); the Center for Inorganic Photovoltaic Materials (NRF-2010-0007692); and the Korea Center for Artificial Photosynthesis (KCAP) funded by the Ministry of Education, Science and Technology (NRF-2009-C1AAA001-2009-0093879).

■ REFERENCES

(1) Oregan, B.; Gratzel, M. *Nature* **1991**, *353*, 737.
(2) Gratzel, M. *J. Photochem. Photobiol. A: Chem.* **2004**, *164*, 3.
(3) Wang, P.; Zakeeruddin, S. M.; Comte, P.; Exnar, I.; Gratzel, M. *J. Am. Chem. Soc.* **2003**, *125*, 1166.
(4) Wang, P.; Zakeeruddin, S. M.; Moser, J. E.; Nazeeruddin, M. K.; Sekiguchi, T.; Gratzel, M. *Nat. Mater.* **2003**, *2*, 402.
(5) Chaban, V. V.; Prezhdo, O. V. *J. Phys. Chem. Lett.* **2011**, *2*, 2499.
(6) Noda, A.; Hayamizu, K.; Watanabe, M. *J. Phys. Chem. B* **2001**, *105*, 4603.
(7) Welton, T. *Chem. Rev.* **1999**, *99*, 2071.
(8) Bonhote, P.; Dias, A. P.; Papageorgiou, N.; Kalyanasundaram, K.; Gratzel, M. *Inorg. Chem.* **1996**, *35*, 1168.
(9) Freire, M. G.; Carvalho, P. J.; Gardas, R. L.; Marrucho, I. M.; Santos, L.; Coutinho, J. A. P. *J. Phys. Chem. B* **2008**, *112*, 1604.
(10) Kawano, R.; Matsui, H.; Matsuyama, C.; Sato, A.; Susan, M.; Tanabe, N.; Watanabe, M. *J. Photochem. Photobiol. A: Chem.* **2004**, *164*, 87.
(11) Seddon, K. R.; Stark, A.; Torres, M. J. *Pure Appl. Chem.* **2000**, *72*, 2275.
(12) Cammarata, L.; Kazarian, S. G.; Salter, P. A.; Welton, T. *Phys. Chem. Chem. Phys.* **2001**, *3*, 5192.
(13) Mikoshiba, S.; Murai, S.; Sumino, H.; Kado, T.; Kosugi, D.; Hayase, S. *Curr. Appl. Phys.* **2005**, *5*, 152.
(14) Tran, C. D.; Lacerda, S. H. D.; Oliveira, D. *Appl. Spectrosc.* **2003**, *57*, 152.
(15) Saha, S.; Hamaguchi, H. O. *J. Phys. Chem. B* **2006**, *110*, 2777.
(16) Chaban, V. V.; Prezhdo, O. V. *Phys. Chem. Chem. Phys.* **2011**, *13*, 19345.
(17) Kawano, R.; Watanabe, M. *Chem. Commun.* **2003**, 330.
(18) Usui, H.; Matsui, H.; Tanabe, N.; Yanagida, S. *J. Photochem. Photobiol. A: Chem.* **2004**, *164*, 97.
(19) Belmares, M.; Blanco, M.; Goddard, W. A.; Ross, R. B.; Caldwell, G.; Chou, S. H.; Pham, J.; Olofson, P. M.; Thomas, C. *J. Comput. Chem.* **2004**, *25*, 1814.
(20) Lin, S. T.; Blanco, M.; Goddard, W. A. *J. Chem. Phys.* **2003**, *119*, 11792.
(21) Thorsmolle, V. K.; Rothenberger, G.; Topgaard, D.; Brauer, J. C.; Kuang, D. B.; Zakeeruddin, S. M.; Lindman, B.; Gratzel, M.; Moser, J. E. *ChemPhysChem* **2011**, *12*, 145.
(22) Mikoshiba, S.; Murai, S.; Sumino, H.; Hayase, S. *Chem. Lett.* **2002**, 1156.
(23) Hahlin, M.; Johansson, E. M. J.; Scholin, R.; Siegbabn, H.; Rensmo, H. *J. Phys. Chem. C* **2011**, *115*, 11996.
(24) Nazeeruddin, M. K.; Kay, A.; Rodicio, I.; Humphrybaker, R.; Muller, E.; Liska, P.; Vlachopoulos, N.; Gratzel, M. *J. Am. Chem. Soc.* **1993**, *115*, 6382.
(25) Zakeeruddin, S. M.; Nazeeruddin, M. K.; Humphry-Baker, R.; Pechy, P.; Quagliotto, P.; Barolo, C.; Viscardi, G.; Gratzel, M. *Langmuir* **2002**, *18*, 952.
(26) Anthony, J. L.; Maginn, E. J.; Brennecke, J. F. *J. Phys. Chem. B* **2001**, *105*, 10942.